Chapter 10

A Numerical Study of Amplification of Space Charge Waves in n-InP Films

Abel García-Barrientos, Francisco R. Trejo-Macotela,
Liz del Carmen Cruz-Netro and Volodymyr Grimalsky

Additional information is available at the end of the chapter

http://dx.doi.org/10.5772/47764

1. Introduction

The millimeter and sub-millimeter microwave ranges are very important for applications in communications, radar, meteorology and spectroscopy. However, the structure of semiconductor devices (transistors, diodes, etc.), required for such a short wavelength, becomes very complex, which makes its fabrication difficult and expensive. One potential alternative to explore the use of such a part of the electromagnetic spectrum resides in the use of non-linear wave interaction in active media. For example, the space charge waves in thin semiconductor films, possessing negative differential conductivity (InP, GaAs, GaN at 300K and strained Si/SiGe heterostructures at 77K), propagate at frequencies that are higher than the frequencies of acoustic and spin waves in solids. This means, for example, that an elastic wave resonator operating at a given frequency is typically 100000 times smaller than an electromagnetic wave resonator at the same frequency. Thus attractively small elastic wave transmission components such as resonators, filters, and delay lines can be fabricated.

The scope of space charge waves' applications is very large, because it can be useful to implement monolithic phase shifters, delay lines, and analog circuits for microwave signals. Space charge waves have been researched since a long time ago, which can be traced back to the 1950s [Benk]. The early experimental work on the amplification of space charge waves with a perturbation field started in the 1970s [Dean] and continues today [Kumabe *et al.* & Barybin *et al.*]. The first monolithic device using space charge waves was a two-port amplifier developed in the beginning of 1970s in the United States. This device contained an *n*-GaAs film on a dielectric substrate, and a couple of source and drain ohmic contacts. A microwave signal applied to the input electrode modulates the electron density under this electrode. These modulations are drifted to the drain and amplified due to the negative

resistance effect. The amplified signal is taken from the output electrode placed near the drain, see Fig. 1a. Obviously, the output signal is maximal when all the waves reach the output electrodes with the same phase [Wang *et al.*]. The majority of devices based on space charge waves are fabricated on GaAs films, although InP is recognized to have superior characteristics compared to GaAs for power generation in the millimeter wave range [Wandinger & Dragoman *et al.*]. The threshold electric field is 3.2 kV/cm for gallium arsenide and 10 kV/cm for indium phosphide. The peak electron drift velocity is about 2.2 x 10^7 cm/s for gallium arsenide and 2.5 x 10^7 cm/s for indium phosphide. The maximum negative differential mobility is about -2400 cm^2/V-s for GaAs and -2000 cm^2/V-s for indium phosphide [Sze]. An electric field in excess of 10 kV/cm applied to an *n*-InP sample causes the differential electron mobility to become negative. To analyze wave phenomena in GaAs films semiconductors, a set of equations to describe the charge transport is commonly used [Kazutaka]. In the case of InP, the same set of equations can be used, because the band structure of InP is very similar to the one of GaAs. In this theory, with small initial perturbations, continuity, momentum and energy equations, and Poisson's equation are solved. The solutions show that the modulations of electron density travel along the beam in the form of waves called space charge waves; these results, for n-GaAs thin films, are in [Grimalsky, *et al.*]. In this paper, the non-linear interaction of space charge waves including the amplification in microwave and millimeter wave range in *n*-InP films, possessing the negative differential conductance phenomenon, is investigated theoretically; also the spatial increment of space charge waves in InP films is compared with the results in GaAs. The results suggest that the increment observed in the gain is due to the larger dynamic range in n-InP than in n-GaAs films, where the optical scattering mechanisms play a drastic role rather than acoustic and ionized impurity scattering.

The study of microwave frequency conversion under negative differential conductivity will be one of the most relevant topics in microelectronics and communications in the coming years, due to the potential it represents in terms of amplification of micro- and millimeter-waves. However, in order to understand the behavior of non-stationary effects, a special attention must be paid to the transverse inhomogeneity, carrier-density fluctuations, in the plane of the film, because it may affect, in a negative way, the non-linear wave interaction. Thus, a creation of effective algorithms and computer programs for simulations of non-linear interaction of space charge waves in semiconductor films, where the effects of non-locality and transverse inhomogeneity should be taken into account, becomes of high importance.

2. The equations for space charge waves

Consider n-InP film placed onto substrate without an acoustic contact. It is assumed that the electron gas is localized in the center of film. The thickness of the n-InP film is $2h < 1$ μm, see Fig. 1a. The coordinate system is chosen as follows: X-axis is directed perpendicularly to the film, the electric field E_0 is applied along Z-axis, exciting and receiving antennas are parallel

to Y-axis. 2D model of electron gas in the *n*-InP film is used. Thus, 2D electron concentration is presented only in the plane $x = 0$. The space charge waves possessing phase velocity equal to drift velocity of the electrons $v_0 = v(E_0)$, $E_0 = U_0/L_z$, are considered, where U_0 is bias voltage, L_z is the length of the film. Generally, a non-local dependence of drift velocity v_d of electrons on the electric field takes place.

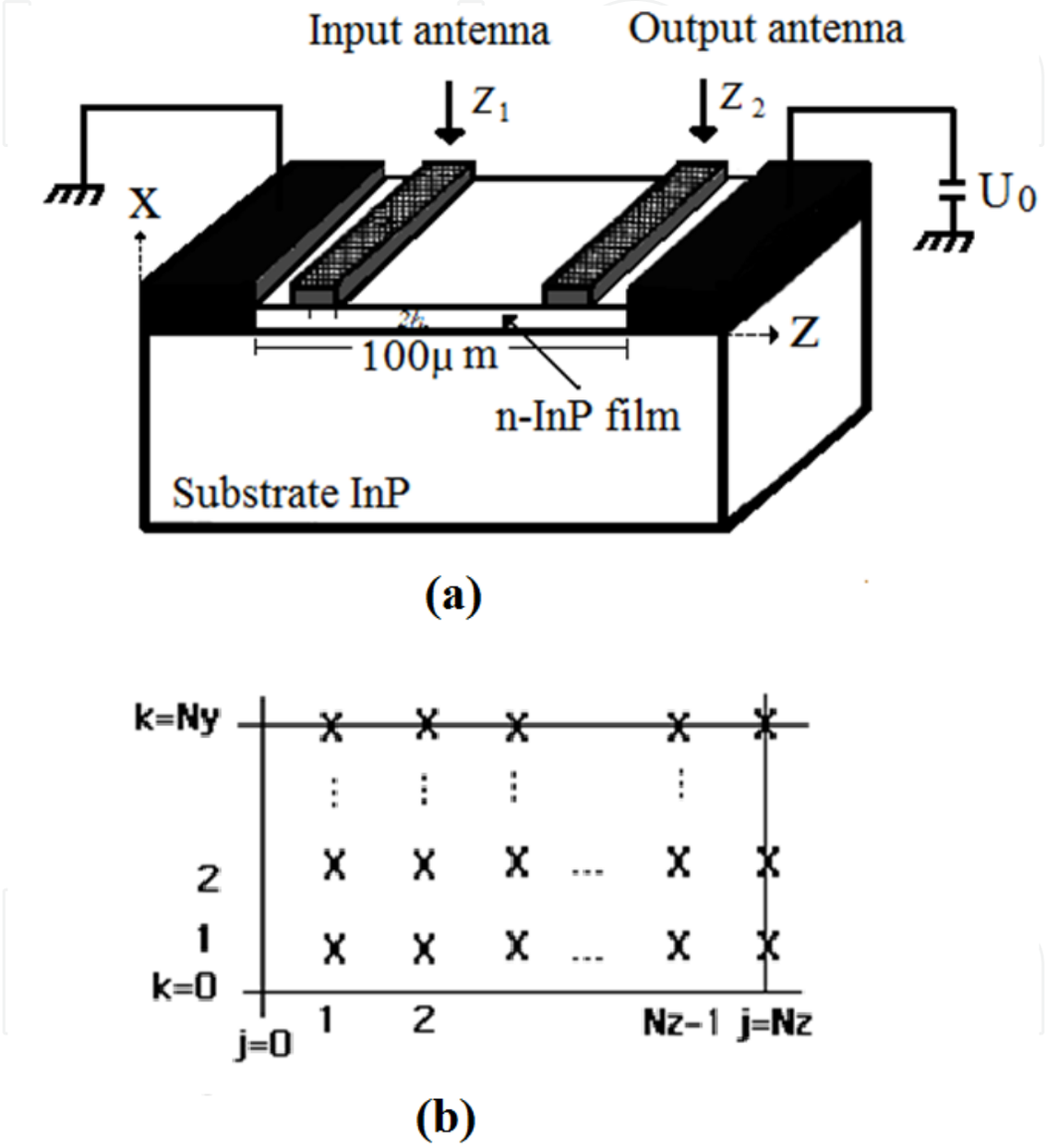

Figure 1. The structure of the *n*-InP traveling-wave amplifier fabricated with an epitaxial layer (a), scheme in device surface for calculating nodes *j* and *k* (b).

In simulations, an approximation of two-dimensional electron gas is used. The set of balance equations for concentration, drift velocity, and the averaged energy to describe the dynamics of space charge waves within the *n*-InP film takes a form, like in GaAs film [Carnez, *et al.*]:

$$\begin{gathered}\frac{d\left(m(w)\vec{v}_d\right)}{dt} = -q\left(\vec{E} - \frac{\vec{v}_d E_s}{v_s}\right)\\ \frac{dw}{dt} = -q\left(\vec{E}\vec{v}_d - E_s v_s\right)\\ \frac{\partial n}{\partial t} + div\left(n\vec{v}_d - D\tilde{N}n\right) = 0\\ D(w) = \frac{2}{3}\frac{\tau_p(w)}{m(w)}\left(w - \frac{1}{2}mv^2\right)\\ \vec{E} = \vec{e}_z E_0 - \tilde{N}\varphi + \vec{e}_z\tilde{E}_{ext}\\ \Delta\varphi = \frac{q}{\varepsilon_0\varepsilon}\left(n - n_0\right)\delta(x)\end{gathered} \tag{1}$$

where v_d is drift velocity, ϕ is the potential, $n = n_0 + \tilde{n}$ where n_0 is constant electron concentration, $\tilde{n}$ is the varying part, w is the electron energy, **D** is the diffusion coefficient, and ε_0 is the lattice dielectric permittivity of *n*-InP, m(w) is averaged effective mass, q is the electron charge, $\tau_{p,w}$(w) are relaxation times, and E_0 is the bias electric field. It should be noticed that the delta function in equation Poisson implicitly defines the density which is important to correctly interpret the equation in actual physical quantities. It is assumed that a condition of occurring negative differential conductivity is realized. Because the signal frequencies are in microwave or millimeter wave range, it is possible to separate diffusion and drift motions. For a sake of simplicity, instead of relaxation times, the parameter E_s is introduced [Carnez *et al.*]:

$$\begin{gathered}\frac{m(w)}{\tau_p(w)} = \frac{E_s}{v_s(E_s)}\\ \frac{w - w_0}{\tau_w(w)} = qE_s v_s(E_s)\end{gathered} \tag{2}$$

In such a representation, the mean energy and effective mass of electron are denoted by w and m(w), the equilibrium value of w is w_0; A direct correspondence between local field dependence and non-local effects is well seen. Because a dependence $E_s = E_s$(w) is unique, it is possible to express the parameters w and v_s through the value of E_s. The dependencies of drift velocity, averaged electron energy and averaged electron mass on electric field in InP films are taken from our Monte Carlo simulation results (see Fig. 2), which are in good agreement with measured data and the set of parameters used in the simulations are very similar from literature [Fischetti].The maximum value of drift velocity in InP is when the electric field is 10 kV/cm, under these high-field conditions some of the electrons can acquire enough energy from the electric field to transfer via inter-valley scattering to the upper valley. Since the mobility of electrons in the upper valley is smaller than in lower valley, the conductivity decreases with increasing field, leading to a negative differential resistance (see Fig. 2a). A comparison of the results for GaAs and InP films reveals that for the field

strength considered most of the electrons in GaAs are in higher valley while in InP less than are transferred. This is due to the difference in the separation of the valleys (0.3 eV in GaAs and 0.6 eV in InP) in spite of the higher field applied in InP [Deb, *et al.*]. A large negative differential conductance appears when increasing electric field more than the threshold fielded; the electrons have not enough energy to make the inter-valley scattering. Beyond this value, the optical scattering mechanisms play a drastic role rather than acoustic and ionized impurity scattering. Since this process is inelastic, the electron energy curves have sensitive variation in its slope; in fact it does not increase as fast as increasing in initial fields (see Fig. 2b).

A small microwave electric signal E_{ext} is applied to the input antenna. When this signal is applied, the excitation of space charge waves in 2D electron gas takes place. These waves are subject to amplification, due to negative differential conductivity. The set of equations (1) form a set of non-linear coupled time dependent partial differential equations. These differential equations are discretized, using a finite-difference scheme and is solved numerically. Calculations are performed for two dimensional grid (see Fig. 1b):

j = 0,1,2,3,…, N_z, along the Z axis.

k = 0,1,2,3,… N_y, along the Y axis.

For potential calculations, we use two dimensional Poisson's equation

$$\frac{\partial^2 \varphi}{\partial y^2} + \frac{\partial^2 \varphi}{\partial z^2} = -\chi \tilde{n} \delta(x) \tag{3}$$

We use the Fast Fourier Transform, the sine transform along the Z axis and cosine transform along the Y axis with boundary conditions:

$$\varphi(x, y, z) = \sum_{j=1}^{N_z} \sum_{k=0}^{N_y} \phi_{jk}(x)\, SinK_{zj} z * CosK_{zj} y \tag{4}$$

$$\varphi|_{z=0} = \varphi|_{z=l_z} = 0;\ \left.\frac{\partial \varphi}{\partial y}\right|_{y=0} = \left.\frac{\partial \varphi}{\partial y}\right|_{y=l_z} = 0; K_{zj} = \frac{\pi k}{l_z}; K_{yk} = \frac{\pi k}{l_y} \tag{5}$$

$$E_y\big|_{y=0} = E_y\big|_{y=l_y} = 0;\ v_y\big|_{y=0} = v_y\big|_{y=l_y} = 0 \tag{6}$$

by replacing the equation (4) in (3) we obtain

$$\frac{d^2 \phi_{jk}(x)}{dx^2} - \left({K_{zj}}^2 + {K_{yk}}^2\right)\phi_{jk}(x) = \frac{d^2 \phi_{jk}(x)}{dx^2} - {\Theta_{\mathrm{jk}}}^2 \phi_{jk}(x) = -\chi \tilde{N}_{jk} \delta(x) \tag{7}$$

now

$$\tilde{n}(y, z) = \sum_{j=1}^{N_z} \sum_{k=0}^{N_y} \tilde{\mathrm{N}}_{jk}\, SinK_{zj} z * CosK_{zj} y \tag{8}$$

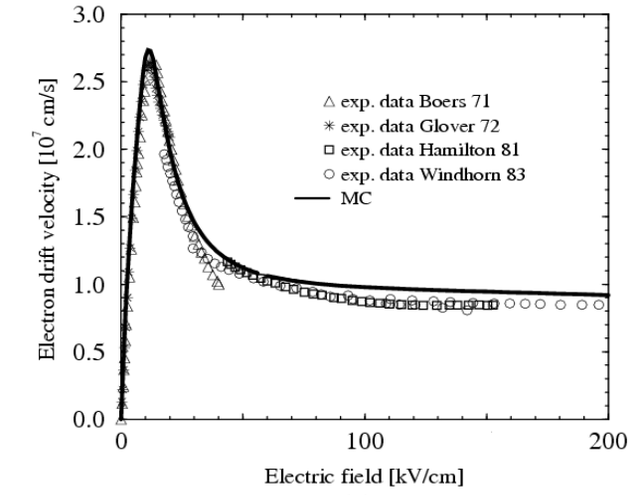

Figure 2. Electron drift velocity (a), average electron energy (b), averaged mass (c) versus electric field used in simulations; (-) MC data, (○) Fischetti, and (□) Gonzalez and experimental data: (Δ) Boers, (*) Glover, (□) Hamilton, and (○) Windhorn.

the solution of equation (7) is in the follow form:

$$\phi_{jk}(x) = \frac{\chi}{2\Theta_{\mathrm{jk}}} \tilde{N}_{jk} e^{-\Theta_{\mathrm{jk}}|x|} \tag{9}$$

For calculations v_z, v_y, E_y and E_z is necessary to calculate first values $y = 0$ y $y = N_y$ ($k = 0$ y $k = N_y$), then we made the same along the Z axis (increasing j) one by one, as shown in Fig. 1b, for each value of j (j = 1.2 3, ..., N_z) is needed to solve a problem with a tridiagonal matrix. In this case, values $v_z|_{z=0} = v_z|_{z=lz} = 0$; $E_z|_{z=0} = E_z|_{z=lz} = 0$ are already known. We can obtain from potential $\tilde{E_z}$ and $\tilde{E_y}$.

$$\varphi(x,y,z) = \frac{\chi}{2} \sum_{j=1}^{N_z} \sum_{k=0}^{N_y} \frac{\tilde{\mathrm{N}}_{jk}}{\Theta_{\mathrm{jk}}} e^{-\Theta_{\mathrm{jk}|x|}} SinK_{zj} z * CosK_{zj} y \tag{10}$$

$$\tilde{E}_z\big|_{x=0} = -\frac{\partial \varphi}{\partial z}\bigg|_{x=0} = -\frac{\chi}{2} \sum_{j=1}^{N_z} \sum_{k=0}^{N_y} \frac{\tilde{\mathrm{N}}_{jk}}{\Theta_{\mathrm{jk}}} K_{zj} CosK_{zj} z * CosK_{yk} y \tag{11}$$

$$\tilde{E}_y\big|_{x=0} = -\frac{\partial \varphi}{\partial y}\bigg|_{x=0} = \frac{\chi}{2} \sum_{j=1}^{N_z} \sum_{k=0}^{N_y} \frac{\tilde{\mathrm{N}}_{jk}}{\Theta_{\mathrm{jk}}} K_{yk} SinK_{zj} z * SinK_{yk} y \tag{12}$$

For $\tilde{E_z}$ we have cosine transform along the Z direction and also for Y axis, and for $\tilde{E_y}$ we have the sine transform in the Z direction and also for Y direction, therefore the program was conducted, the Fourier transform of the sine in the Z direction and in the Y direction cosine transform for $\tilde{n}(y,z)$, and for calculations φ_{jk} (x=0) we use the Inverse Fast Fourier Transform (IFFT). We use the IFFT (Sine-Cosine) for calculations φ(x=0), and for $\tilde{E_z}$ we used the IFFT (Cosine - Cosine) and for $\tilde{E_y}$ we used the IFFT (Sine - Sine).

For calculations v_z we use equation (1), replacing the partial derivatives by their equations in difference

$$\frac{(mv_z)_{j,k}^{p+1} - (mv_z)_{j,k}^{p}}{\tau} + (v_z)_{j,k}^{p+1} \frac{(mv_z)_{j,k}^{p+1} - (mv_z)_{j-1,k}^{p+1}}{h_z} + (v_z)_{j,k}^{p+1} \frac{(mv_z)_{j,k+1}^{p+1} - (mv_z)_{j,k-1}^{p+1}}{2h_y} = \gamma_2 \left[(E_z)_{j,k}^{p+1} - \left(\frac{E_s}{v_s}\right)_{j,k}^{p+1} (v_z)_{j,k}^{p+1} \right] \tag{13}$$

ordering the terms to get a system from equation (13)

$$\alpha_{-1}(v_z)_{j,k-1}^{p+1} + \alpha_0 (v_z)_{j,k}^{p+1} + \alpha_{+1}(v_z)_{j,k+1}^{p+1} = f_k \tag{14}$$

This difference equation is only for j = 1,2,3,…,N_z and for k = 1,2,3,…,N_y – 1 forming a tridiagonal matrix system, because for $y = 0$ or $y = l_y$ ($k = 0$ o $k = N_y$) $v_y = 0$. Furthermore, if we substitute for $y = 0$, equation (13) is like in the case of one dimension so we can obtain:

$$(v_z)_{j,0}^{p+1} = \frac{(mv_z)_{j,0}^{p} + \gamma_2 \tau (E_z)_{j,0}^{p+1}}{m_{j,0}^{p+1} + \frac{\tau}{h_z}\left((mv_z)_{j,0}^{p+1} - (mv_z)_{j-1,0}^{p+1}\right) + \gamma_2 \tau \left(\frac{E_s}{v_s}\right)_{j,0}^{p+1}} \tag{15}$$

And the same form for $(v_z)_{j=0,Ny}^{p+1}$, we take into account $(v_z)_{j=0,k}^{p+1} = v_s(E_0)$ from boundary conditions. And for calculations v_y, in the same form like v_z

$$\frac{(mv_y)_{j,k}^{p+1} - (mv_y)_{j,k}^{p}}{\tau} + (v_y)_{j,k}^{p+1} \frac{(mv_z)_{j,k}^{p+1} - (mv_z)_{j-1,k}^{p+1}}{h_z} + (v_y)_{j,k}^{p+1} \frac{(mv_y)_{j,k+1}^{p+1} - (mv_y)_{j,k-1}^{p+1}}{2h_y} = \gamma_2 \left[(E_y)_{j,k}^{p+1} - \left(\frac{E_s}{v_s}\right)_{j,k}^{p+1} (v_y)_{j,k}^{p+1} \right] \tag{16}$$

$$-\frac{\tau}{2h_y} m_{j,k-1}^{p+1} (v_y)_{j,k}^{p+1} (v_y)_{j,k-1}^{p+1} + \left[m_{j,k}^{p+1} \left(1 + \frac{\tau}{h_z} (v_z)_{j,k}^{p+1} + \gamma_2 \tau \left(\frac{E_s}{v_s}\right)_{j,k}^{p+1} \right) \right] (v_y)_{j,k}^{p+1} + \frac{\tau}{2h_y} m_{j,k+1}^{p+1} (v_y)_{j,k}^{p+1} (v_y)_{j,k+1}^{p+1} = (mv_y)_{j,k}^{p} + \frac{\tau}{h_z} (v_z)_{j,k}^{p+1} (mv_y)_{j-1,k}^{p+1} + \gamma_2 \tau (E_y)_{j,k}^{p+1} \tag{17}$$

also $(v_y)_{j,0}^{p+1} = (v_y)_{j,N_y}^{p+1} = 0$.

for calculations n, we use the continuity equation in two dimensions, with their respective boundary conditions, also to make it easier the calculations we use operators

$$\frac{\partial n}{\partial t} + \frac{\partial}{\partial z}\left(v_z n - D(w) \frac{\partial n}{\partial z} \right) + \frac{\partial}{\partial y}\left(v_y n - D(w) \frac{\partial n}{\partial y} \right) = \frac{\partial n}{\partial t} + \hat{A}_z n + \hat{A}_y n = 0 \tag{18}$$

$$n|_{z=0} = n|_{z=l_z} = n_0 \quad \text{and} \quad \left.\frac{\partial n}{\partial y}\right|_{y=0} = \left.\frac{\partial n}{\partial y}\right|_{y=l_y} = 0 \tag{19}$$

where $\hat{A}_z$ y $\hat{A}_y$ are operators and dependent from v_z, v_y and D, and they are defined as:

$$\hat{A}_z n = \frac{\partial}{\partial z}\left(v_z n - D(w) \frac{\partial n}{\partial z} \right) \text{ and } \hat{A}_y n = \frac{\partial}{\partial y}\left(v_y n - D(w) \frac{\partial n}{\partial y} \right) \tag{20}$$

we use the approximation

$$\frac{\frac{3}{2} n^{p+1} - 2n^{p} + \frac{1}{2} n^{p-1}}{\tau} + \hat{A}_z n + \hat{A}_y n = 0 \tag{21}$$

A transverse inhomogeneity of the structure in the plane of the film along Y axis is taken into account. The following parameters are chosen: 2D concentration of electrons in the film is $n_0 = 5\text{x}10^{14}$ cm^{-2}, the initial uniform drift velocity of electrons is $v_0 = 2\text{x}10^{7}$cm/s, the length of the film is $l_z = 0.1$ mm, the thickness of the film is $2h = 0.1$ - 1 μm.

3. Spatial increment of space charge waves

In this section, a description of propagation of longitudinal space charge waves in a negative differential conductance medium, using the drift - diffusion equations to find the dispersion relation, is presented; the equation of continuity (22) and Poisson's equation (23) for electrons are

$$\frac{\partial n}{\partial t}+\frac{\partial}{\partial z}\left[v(E_z|_{x=0})n-D\frac{\partial n}{\partial z}\right]=0 \tag{22}$$

$$\Delta\varphi=-\frac{q}{\varepsilon_0\varepsilon}(n-n_0)\delta(x) \tag{23}$$

where n is the surface concentration, n_0 is the equilibrium density, D is the diffusion constant and $E_z=-\frac{\partial\varphi}{\partial z}$. Let us introduce $n=n_0+\tilde{n}$, $\varphi=\varphi_0+\tilde{\varphi}$ and $E=E_0+\tilde{E}_s$, with E_0 equal to the *dc* (direct current) applied field, and $\tilde{E}_s$ is the *rf* (radio frequency) field, with some approximations and mathematical tools the equations (22) and (23) can be written as

$$\frac{\partial\tilde{n}}{\partial t}+\frac{\partial}{\partial z}\left[v_0\tilde{n}+\frac{dv}{dE}n_0\tilde{E}_s-D\frac{\partial\tilde{n}}{\partial z}\right]=0 \tag{24}$$

$$\Delta\tilde{\varphi}=-\frac{q}{\varepsilon_0\varepsilon}(\tilde{n})\delta(x) \tag{25}$$

If one assumes that $\tilde{n}=\tilde{N}exp(-i\omega t+ikz)$ and $\tilde{\varphi}=\phi(x)exp(-i\omega t+ikz)$, then

$$\tilde{N}\left(-i\omega+ikv_0+Dk^2+ik\frac{dv}{dE}n_0\tilde{E}\big|_{x=0}\right)=0 \tag{26}$$

$$\frac{d^2\phi}{dx^2}-k^2\phi=-\frac{q}{\varepsilon_0\varepsilon}\tilde{N}\delta(x) \tag{27}$$

The equation (27) is equivalent to:

$$\frac{d^2\phi}{dx^2}-k^2\phi=0 \text{ for } x\neq 0 \tag{28}$$

$$\left.\frac{d\phi}{dx}\right|_{x=+0}-\left.\frac{d\phi}{dx}\right|_{x=-0}=-\frac{q}{\varepsilon_0\varepsilon}\tilde{N} \tag{29}$$

ϕ is continuous at $x = 0$. A proposed solution is

$$\phi=\begin{cases}Aexp(-kx), x>0\\ Bexp(kx), x<0\end{cases} \tag{30}$$

If $\phi|_{x=+0}=\phi|_{x=-0}$ then A=B and

$$\tilde{\varphi}=\frac{q}{\varepsilon_0\varepsilon}\frac{\tilde{n}}{2k}exp(-k|x|) \tag{31}$$

then

$$\tilde{E}_z\big|_{x=0} = -ik\tilde{\varphi}|_{x=0} = -i\frac{q\tilde{n}}{2\varepsilon_0\varepsilon} \tag{32}$$

If one substitutes the equation (32) into the equation (26) one obtains

$$\tilde{N}(-i\omega + ikv_0 + Dk^2) + ik\frac{dv}{dE}n_0\frac{(-i)q\tilde{N}}{2\varepsilon_0\varepsilon} = 0 \tag{33}$$

or

$$\omega = v_0k - iDk^2 - i\frac{qn_0}{2\varepsilon_0\varepsilon}\frac{dv}{dE}k \tag{34}$$

Using the Drift-Diffusion equation, a study about of how a small, periodic disturbance may propagate in this InP film has been introduced by means the dispersion equation D(ω,k) = 0, because it determines the modes of propagation, their phase velocities and group velocities and also show if any instability can exists. For our present purpose, which is when the negative differential conductivity shows up, dv/dE < 0, space charge waves will get amplified instead of being damped. In general, we consider the cases where $\omega = 2\pi f$ is real and $k = k' + ik''$ has real and imaginary part. The case $k'' > 0$ corresponds to spatial increment (amplification), whereas the case $k'' < 0$ corresponds to the decrement (damping). In Fig. 3, the spatial increment of space charge waves in an n-InP film is shown in the curve 2, where the electron concentration is n_0 = 0.8 x 10^{14} cm^{-2}, the bias electric field is E_0 = 20 kV/cm. In curve 3, the electron concentration is n_0 = 5 x 10^{14} cm^{-2} with the same bias electric field, E_0 = 20 kV/cm. Curve 1 is the result for n-GaAs films where the electron concentration is n_0 = 5 x 10^{14} cm^{-2} and the bias electric field is E_0 = 4.5 kV/cm. The stationary values of E_0 have been chosen in the regime of negative differential conductivity (dv/dE <0) for all cases. One can see that an amplification of space charge waves in InP films occurs in a wide frequency range, and the maximal spatial increment is k'' = 3x10^5 m^{-1} at the frequency f = 35 GHz. When compared

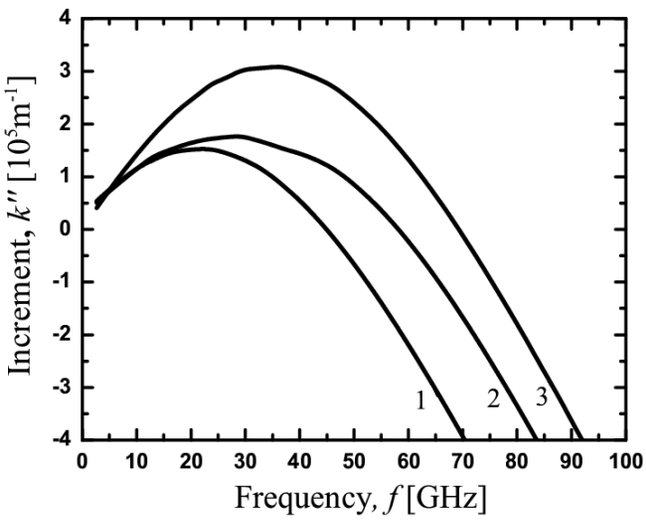

Figure 3. Spatial increments of instability $k''(f)$ of space charge waves. Curve 1 shows results for an n-GaAs film [Garcia-B. *et al.*]. Curve 2 is for InP films with E_0 = 20 kV/cm, n_0 = 0.8x10^{14} cm^{-2} and film thickness 2h = 0.05 μm and curve 3 is for the electron concentration is n_0 = 5 x 10^{14} cm^{-2} with the same bias electric field, E_0 = 20 kV/cm.

with a case of the GaAs film, it is possible to observe an amplification of space charge waves in InP films at essentially higher frequencies $f > 44$ GHz. To obtain an amplification of 25 dB, it is necessary to use a distance between the input and output antennas of about 0.09 mm.

4. Results and simulation

The propagation and amplification of space charge waves in *n*-GaAs thin films with negative difference conductance have been studied in the last decade [Mikhailov *et al.*], however *n*-InP films have not been addressed yet, and are subject of this work. We address the device presented in Fig. 1 by means of numerical simulations. An *n*-InP epitaxial film of thickness 0.1 - 1 μ*m* is put on an InP semi-insulating substrate. The two-dimensional electron density in the film is chosen to be $n_0 = 5 \times 10^{14}$ cm^{-2}. On the film surface are the cathode and anode ohmic contacts (OCs), together with the input and output coupling elements (CEs). Designed as a Schottky-barrier strip contacts, the CEs connect the sample structure to microwave sources. A dc bias voltage (above the Gunn threshold, 20 kV/cm) was applied between the cathode and anode OCs, causing negative differential conductivity in the film. The CEs perform the conversion between electromagnetic waves and space charge waves, where the excitation of space charge waves in the 2D electron gas takes place. In the simulations an approximation of two-dimensional electron gas is used.

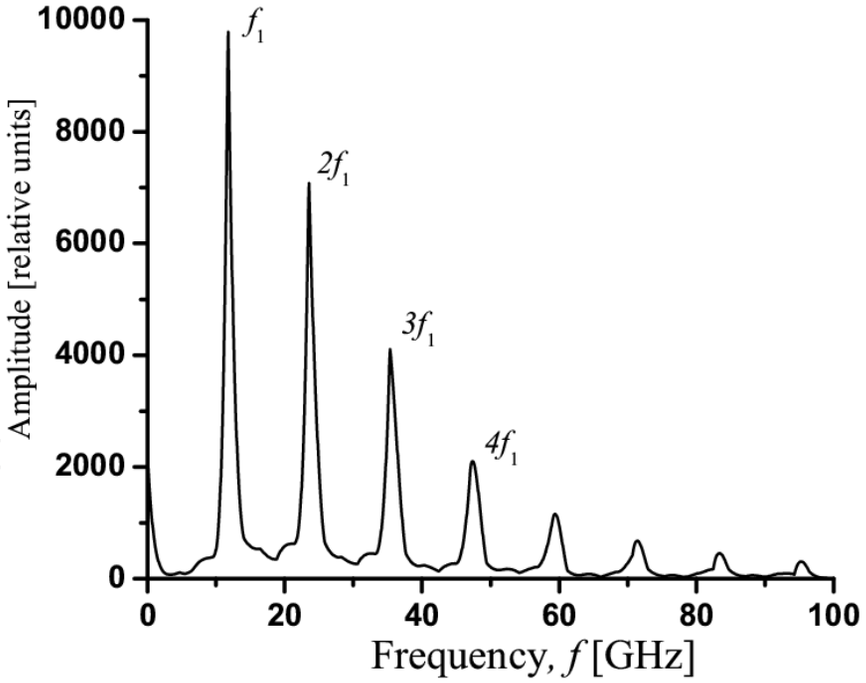

Figure 4. Spectral components of the electric field of space charge waves. The effective excitation of harmonics is presented. The input carrier frequency is $f = 12$ GHz.

A small microwave electric signal $E_{ext} = E_m \cdot \sin(\omega t) \cdot \exp(-((z-z_1)/z_0)^2-((y-y_1)/y_0)^2)$ is applied to the input antenna. Here z_1 is the position of the input antenna, z_0 is its half-width. Therefore, the parameter $2t_0$ determines the duration of the input electric pulse. In our simulations, this parameter is $2t_0 = 2.5$ ns. The carrier frequency f is in the microwave range: $f = 1$ GHz – 100

GHz. When a small microwave signal is applied to the input antenna, the excitation of space charge waves in the 2D electron gas takes place. The space charge waves are subject to amplification, due to the negative differential conductivity. The stable implicit difference scheme is used. The following parameters have been chosen: 2D electron concentration in the film is $n_0 = 5\text{x}10^{14}$ cm^{-2}, the initial uniform drift velocity of electrons is $v_0 \approx 2\text{x}10^7$ cm/s (E_0 =15 – 20 kV/cm), the length of the film is $L_z = 0.1$ mm, the thickness of the film is $2h = 0.1$ - 1 μm. The typical output spectrum of the electromagnetic signal is given in Fig. 4. The input carrier frequency is $f = 12$ GHz. The amplitude of the input electric microwave signal is E_m = 25V/cm. Although the growth rate decreases as the rf frequency increases, for our case an amplification of 25 dB is obtained. The maximum of the input pulse occurs at $t_1 = 2.5$ ns. One can see both the amplified signal at the first harmonic of the input signal and the harmonics generations of the input signal, which is generated due to the non-linearity of space charge waves.

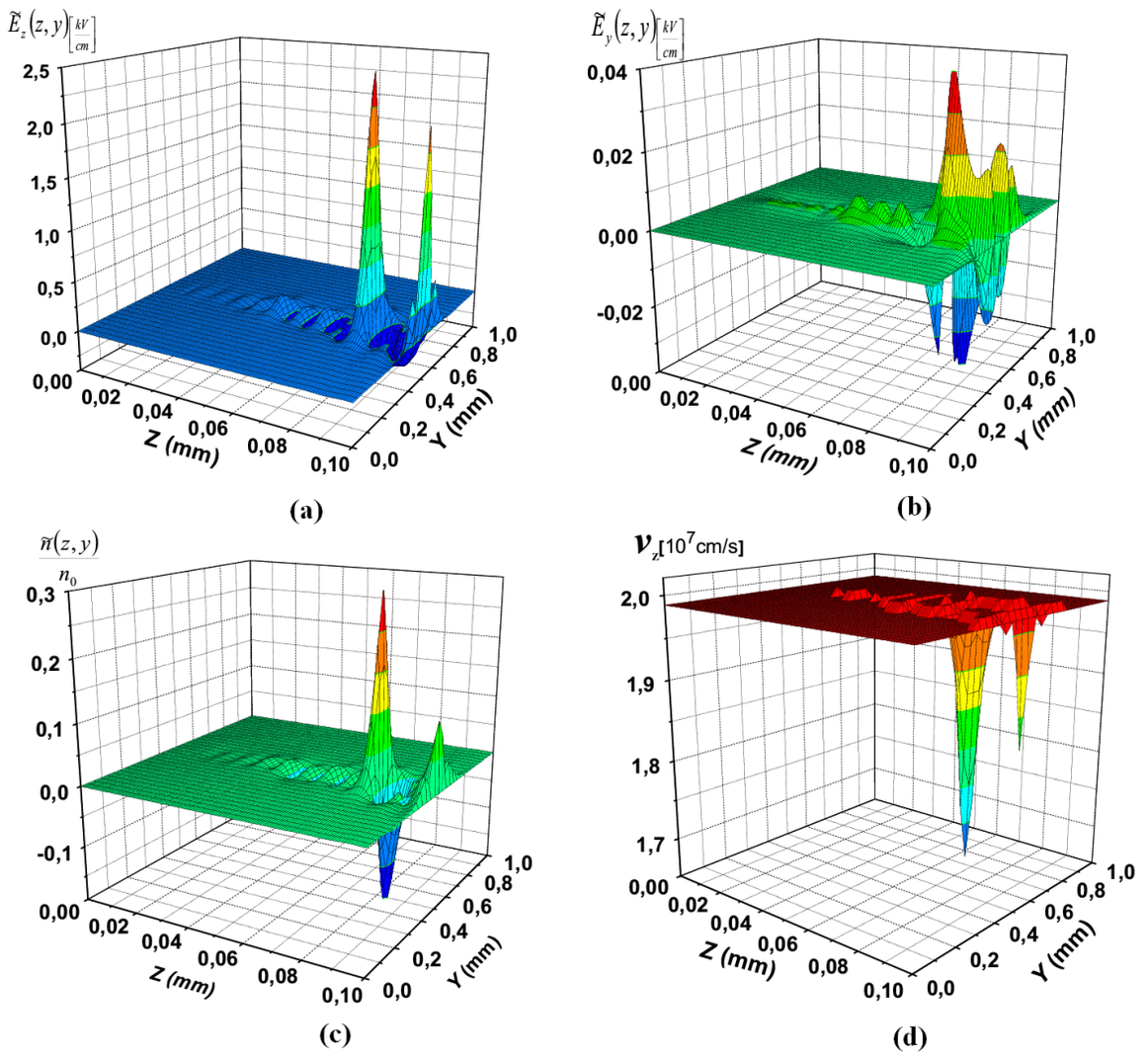

Figure 5. The spatial distributions of the alternative part of the electric field component $E\tilde{}_z$ of space charge wave (a); the component of electric field $E\tilde{}_y$ (b); alternative part of the electron concentration $n\tilde{}$ (c); and the component of the electron drift velocity v_z (d). The length of the film is 0.1 mm. The transverse width of the film along Y axis is 1 mm.

The spatial distributions of the alternate component of the electric field $E\tilde{}_z$, $E\tilde{}_y$, the alternate part of the electron concentration $\tilde{n}$, and the drift velocity v_z are given in Fig. 5, at the time moment t = 4 ns. One can see the maximum variations are in the output antenna and the spatial distribution in direction $E\tilde{}_z$ is bigger than in $E\tilde{}_y$, it is because the propagation of space charge wave. The length of the film is 0.1 mm. The transverse width of the film along Y axis is 1 mm. The duration of the input electric pulse is 2.5 ns. The spatial distributions are presented for the time moment 1.5 ns after the maximal value of the input signal. Direct numerical simulations have confirmed pointed below results on linear increments of space charge waves amplification. Also a possibility of non-linear frequency doubling and mixing is demonstrated. To get the effective frequency doubling in the millimeter wave range, it is better to use the films with uniform doping.

5. Conclusions

A theoretical study of two-dimensional amplification and propagation of space charge waves in n-InP films is presented. A microwave frequency conversion using the negative differential conductivity phenomenon is carried out when the harmonics of the input signal are generated. A comparison of the calculated spatial increment of instability of space charge waves in n-GaAs and n-InP films is performed. An increment in the amplification is observed in InP films at essentially higher frequencies f > 44 GHz than in GaAs films, which is due to its larger dynamic range. The maxi mum amplification (gain of 25 dB) is obtained at f = 35 GHz, using a distance between the input and output antennas of about 0.09 mm.

Author details

Abel García-Barrientos and Francisco R. Trejo-Macotela
Polytechnic University of Pachuca, Hidalgo, Mexico

Liz del Carmen Cruz-Netro
Polytechnic University of Altamira, Tamaulipas, Mexico

Volodymyr Grimalsky
Autonomous University of Morelos, Cuernavaca, Morelos, Mexico

Acknowledgement

This project has been partially funded by the CONACyT- Mexico grant CB-169062 and by the ECEST-SEP (Espacio Común de Educación Superior Tecnológica) Program under the mobility program for professors.

6. References

Barybin A.A., Mikhailov A.I., Parametric interaction of space-charge waves in asymmetric thin-film n-GaAs structures, Tech. Phys.,vol. 48, no. 6, pp. 761 – 767, 2003.

Beck A.H.W, Space-charge waves and slow electromagnetic waves, Pergamon, New York, 1958.

Boers P.M., Measurements on the velocity/field characteristics of indium phosphide, Electron.Lett., vol. 7, no.20, pp. 625-626, 1971.

Carnez B., Cappy A., Kaszynskii A., Constant E. and Salmer G., Modeling of submicrometer gate FET including effect of nonstationary dynamics, J. Appl. Phys., vol. 5, no. 1, pp. 784-790, 1980.

Dean R.H, Travelling-wave amplifier using epitaxial GaAs layer, Electron. Lett., vol. 6, no. 24, pp.775, 1970.

Deb Roy M. and Nag B. R., Velocity auto-correlation and hot-electron diffusion constant in GaAs and InP, Appl. Phys. A, vol. 28, 1982.

Dragoman M., Block M., Kremer R., Buchali F., Tegude F. J., and Jager D., Coplanar microwave phase shifter for InP-based MMICs, Microelectronics Engineering, vol. 19, pp. 421-424, 1992.

Fischetti M.V., Monte Carlo simulation of transport intechnologically significant semiconductors of thediamond and zinc-blende structures-Part I:homogeneous transport, IEEE Transactions on Electron Devices, vol. 38, no. 3**,** 1991.

Garcia-B. A., Grimalsky V., Gutierrez-D. E. A. and Palankovski V., Non-stationary effects of space charge in semiconductor films, J. Appl.Phys., vol. 105, no. 7, pp. 1-6, 2009.

Glover G.H., Microwave measurement of the velocity-field characteristic of n- type InP, Appl. Phys. Lett., vol. 20, pp. 224-225, 1972.

Gonzalez Sanchez, T., Velazquez Perez J. E., Gutierrez Conde P. M., and Pardo D., Electron transport in InP under high electric field conditions, Semicond. Sci. Technol.vol. 7, no. 1, 1992.

Grimalsky V., Gutierrez-D. E., Garcia-B A.. and Koshevaya S., "Resonant excitation of microwave acoustic modes in n-GaAs film, Microelectronics Journal, vol. 37, pp. 395-403 (2006).

Hamilton D.K., Measurements of dipole domains in indium phosphide using a new point-contact probe, Proc. IEE Solid-State and Electron Devices, vol. 128, no. 2, pp. 6167, 1981.

Kazutaka T., Numerical Simulation of Submicron Semiconductor Devices, London, Artech House, pp. 171-189, 1993.

Kumabe K. and Kanbe H., GaAs travelling-wave amplifier, Int. J. Electronics, vol. 58, no. 4, pp. 587-611, 1985.

Mikhailov A.I., Experimental study of the parametric interaction between space-charge waves in thin-film GaAs-based semiconductor structures, Tech. Phys. Lett.,vol. 26, no. 3, pp. 217 – 219, 2000.

Sze S. M., High Speed Semiconductor Devices, Wiley, New York, 1992.

Wandinger L., mm-Wave InP Gunn devices: Status and trends, Microwave J., vol. 24, no. 3, pp. 71 - 78, 1981.

Wang Y. and Jahandoots H., Solid-stated traveling-wave amplifiers based on multistream instability, Int. J. Electronics, vol. 58, no. 4, pp. 571-585, 1985.

Windhorn T.H., Cook L.W., Haase M.A., and Stillman G.E., Electron transport in InP at high electric fields, Appl. Phys. Lett., vol. 42, no. 8, pp. 725-727, 1983.